PCCP

RSC Publishing

COMMUNICATION

View Article Online
View Journal | View Issue

Uniform gold spherical particles for single-particle surface-enhanced Raman spectroscopy†

Cite this: *Phys. Chem. Chem. Phys.*, 2013, **15**, 4130

Received 31st October 2012,
Accepted 16th January 2013

DOI: 10.1039/c3cp43857k

www.rsc.org/pccp

Hai-Xin Lin,‡[a] Jie-Ming Li,‡[a] Bi-Ju Liu,[a] De-Yu Liu,[a] Jinxuan Liu,[b] Andreas Terfort,[c] Zhao-Xiong Xie,[a] Zhong-Qun Tian[a] and Bin Ren*[a]

Surface-enhanced Raman spectroscopy (SERS) benefits from the enhanced electromagnetic field of the localized surface plasmon resonance effect of metallic (especially coinage metals) nanoparticles or nanostructures. The detection sensitivity and reproducibility of SERS measurement appear to be the two critical issues in SERS. To solve the problem associated with traditional nanoparticle aggregates and SERS substrates, we propose in this work single particle SERS. We prepared uniform gold microspheres with controllable size and surface roughness using an etching-assisted seed-mediated method. Single particle dark-field spectroscopy and SERS measurements show that particles with a larger roughness give a stronger SERS signal, but still retain a good reproducibility. This study points to the promising future of the practical application of the single particle SERS technique for trace analysis.

Surface-enhanced Raman spectroscopy (SERS) is currently receiving exponentially increased interest, mainly benefiting from the fast development of nanoscience and nanotechnology, as well as Raman instruments, as a result of the shrinking size of lasers and detectors.[1–4] SERS is a unique vibrational technique that can provide the fingerprint of the sample with a high detection sensitivity down to single molecule level.[1–5] It has found applications in fields, such as surface and interface analyses and material, biological, and medical related trace analysis.[1–4] The main SERS activity can be divided into two categories: the application of SERS for analytical purposes and the preparation of different types of SERS substrates to achieve high detection sensitivity or signal reproducibility.[1–4] An increasing number of publications concerning SERS substrates indicates that this field is still far from mature. As far as we know, to date, there is no ideal SERS substrate that can have both a strong signal and good reproducibility, which is the prerequisite for a wider and practical application of SERS. Therefore, any effort that can make a step forward addressing this issue is highly welcomed by the field.[6–9]

It is well-known that the SERS effect is dominantly contributed to by electromagnetic enhancement effects.[10,11] Single molecule SERS studies have invoked intense investigation of the SERS mechanism. It was found that simple metal nanoparticles can usually only produce a very weak SERS enhancement, and the coupled nanoparticles can produce a gigantic enhancement of several orders of magnitude higher than that of the single nanoparticles.[12–15] As a result, there are a lot of efforts to synthesize, by chemical methods with a high yield, highly SERS active nanoparticle aggregates, such as dimer, trimer, or more complex core–satellite nanoparticles or COIN.[16,17] Usually these nanoparticles are very isotropic. As a result, a huge difference in the SERS intensity may be observed when the nanoparticles are aligned in a different orientation to the polarization of the laser light. Except for application in the bulk solution where the signals are averaged over different orientations, the immobilization of such types of complex nanoparticles on a solid SERS substrate will lead to a bad reproducibility. An alternative way to make use of the coupling effect[18] is to prepare two-dimension (2D) nanoparticle arrays and use them as the SERS substrate to obtain a high density of "hot spots" (the region with a high intensity of electromagnetic field).[19–21] However, at present it is still very challenging and time-consuming to obtain a uniform 2D array. The problems existing in the dimer and trimer substrates, are also associated with the 2D substrates.

On the other hand, if we are able to synthesize SERS-active spherical particles with a size comparable to the laser focal spot of the Raman instrument, then the SERS measurement can be

[a] *State Key Laboratory of Physical Chemistry of Solid Surfaces and Department of Chemistry, College of Chemistry and Chemical Engineering, Xiamen University, Xiamen, China. E-mail: bren@xmu.edu.cn; Fax: +86-592-2181906; Tel: +86-592-2186532*

[b] *Institute of Functional Interfaces, Karlsruhe Institute of Technology, Hermann-von-Helmholtz-Platz 1, B 330, Eggenstein-Leopoldshafen D-76344, Germany*

[c] *Institute of Inorganic and Analytical Chemistry, Goethe-University Frankfurt am Main, Frankfurt 60438, Germany*

† Electronic supplementary information (ESI) available: Details of materials and methods, sample preparation and charaterization, the conditions for SERS and scattering spectra measurement, illustration of the proposed mechanism, statistical diagram of particle size, supplementary SEM and HR-TEM images. See DOI: 10.1039/c3cp43857k

‡ These authors contributed equally to this article.

done over one microsphere. Such a microsphere is large enough to be easily identified with a dark field microscope equipped with a Raman instrument. Due to the symmetric feature of microspheres, the SERS signal obtained will no longer depend on the orientation of the microsphere and the polarization of the laser, and the uncertainty in the SERS measurement can be essentially removed. It may greatly help improve the reproducibility in SERS analysis. The key to single particle analysis is the enhancement effect of each individual single particle. As stated above, a smooth particle can only give a very small enhancement effect. However, if one introduces some irregularities or roughness onto the particle surface, such as edges, tips, corners on the nanometer scale, the enhancement effect may be significantly improved.[10,11] It should be noted that, the concept of doing single particle analysis is not new and there are some attempts to prepare highly SERS-active single nanoparticle aggregates by self-assembly[22] or self-aggregation[23,24] methods. However, it is still a great challenge for these methods to obtain highly uniform particles. At least, to date, there are only a few reports concerning the signal reproducibility in the SERS detection using single particles.[22] In this work, we intend to obtain Au spherical particles with reasonably good SERS activity and good reproducibility.

An Au sphere with a very high symmetry could be directly achieved by a one-step method (OM). In this method, cetyltrimethylammonium bromide (CTAB) was used as a capping agent, and the $HAuCl_4$ precursor was reduced by ascorbic acid. The reducing activity of AA and the nucleation rate of Au can be improved by increasing the pH of the solution using $NH_3{\cdot}H_2O$, similar to the role of NaOH.[23] Although microspheres with an almost perfect spherical shape can be obtained, the size distribution is too large to ensure a good reproducibility for SERS measurement (Fig. 1a and Fig. S4a, ESI†). Therefore, an alternative way to synthesize Au microspheres with a narrow size distribution should be pursued.

Seed-mediated methods (SM) have been widely used to prepare uniform single-crystals[25] or twinned-crystals[26] without a secondary nucleation. In this method, the final particles are obtained by assembly of small nuclei from the prior nucleation step over the seeds to minimize surface energy. We attempted to employ this method to obtain more monodispersed Au particles using very uniform Au nanocubes with a 55 nm edge length as the seeds (Fig. S1, ESI†). The SEM image of the large synthesized particles is shown in Fig. 1b. Unfortunately, from the image, one can find that there is a wide size and shape distribution and the histogram created using SEM images gives two peaks (Fig. S4b, ESI†). According to the growing mechanism of SM, if all nuclei are only attached on the seeds instead of self-aggregation, one should be able to obtain monodispersed particles. This is the key to preparation of monodispersed particles. However, if self-aggregation also occurs during the synthesis process, one may obtain two types of particles.[27,28] Accordingly, the peak at around 130 nm can be attributed to the particles formed by attaching nuclei onto the seeds, and the peak at around 65 nm should be attributed to the particles formed by self-aggregation of nuclei without the cubic seeds.

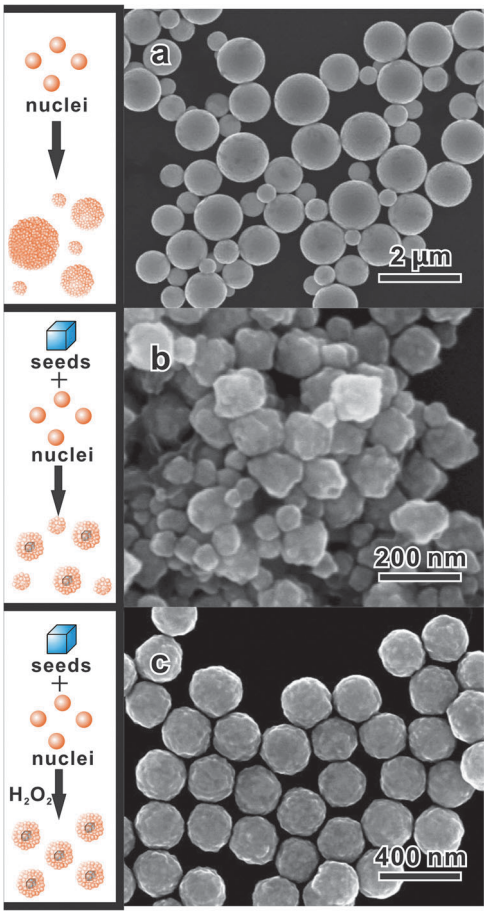

Fig. 1 SEM images of Au spheres synthesized by an (a) one-step method (OM); (b) seed-mediated method (SM); (c) etching-assisted seed-mediated method (EM).

Self-aggregation is a limiting problem that obstructs the adoption of SM to prepare particles through the self-aggregation mode with an ideal size distribution.

Therefore, the key issue is how to prevent the self-aggregation of nuclei. It has been reported that some oxidation agents, such as O_2/Cl^- can selectively etch the twinned nuclei with a high energy defect site, leaving the stable single crystal nuclei.[29,30] Similarly, the nuclei or oligomers have a high specific surface area and when they are dispersed in solution, they have a much higher energy than when attached on the seeds. If we can choose an oxidation agent that may selectively etch the free-standing nuclei or oligomers, we will be able to regulate the self-assembly process and prevent the agglomeration of nuclei in the absence of seeds (Fig. S2, ESI†). For this purpose, we chose H_2O_2 as a regulative etching agent, to allow the nuclei to selectively assemble only on seeds, which leads to the formation of highly uniform spherical particles. The SEM image (Fig. 1c) shows highly uniform Au spheres, with a diameter of about 265 nm.

In order to find out the effect of the size distribution on the SERS activity and reproducibility in SERS measurements, we performed a comparative study on the Au spheres prepared by OM and EM. The UV-vis spectrum (Fig. 2a) of Au spheres prepared by OM shows a broad peak, which is consistent with

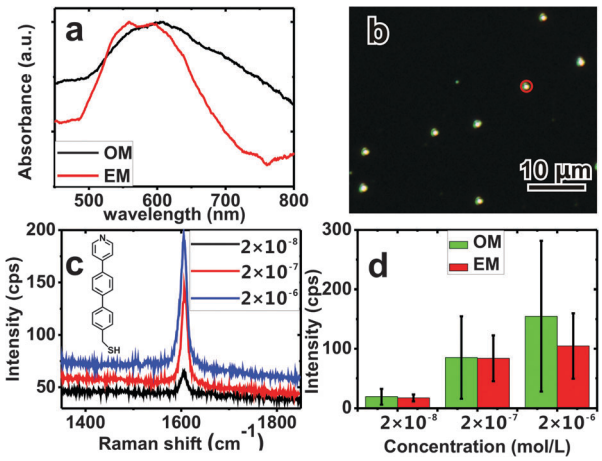

Fig. 2 (a) The UV-vis spectrum of Au spheres prepared by EM and OM. (b) A dark-field image of Au spheres prepared by EM for single particle SERS detection. The red circle stands for the laser focus with a 2 μm diameter. (c) SERS signals obtained for EM-prepared single particles with adsorbed PBT in different PBT concentrations. The inserted molecular structure is PBT. (d) The reproducibility of the SERS signal.

the large size distribution from the SEM image in Fig. 1a; whereas the EM prepared Au spheres give a narrower absorption peak, indicating a narrow size distribution, as seen from Fig. 1c. The Au spheres prepared by both methods are large enough to be conveniently observed with a dark-field microscope, and meanwhile also give a reasonable SERS enhancement to allow single particle SERS measurement. The dark-field and Raman experiments were performed on an inverted Renishaw inVia system, equipped with a dark-field microscope and home-built dark-field spectroscopy. The laser wavelength was 632.8 nm and the laser spot on the sample is about 2 μm. In order to perform single particle SERS measurement, we chose (4′-(pyridin-4-yl)-biphenyl-4-yl)methanethiol (PBT)[31] as a probe molecule. It does not absorb and show the resonant Raman effect in the visible light range. Most importantly it is very stable under our measuring conditions. We first mixed the sol of cleaned particles with PBT solutions. Then a droplet of the mixture was drop-casted onto a hydrophilic silicon wafer. After the solvent was evaporated, the silicon wafer was observed with a white-light dark-field microscope. It should be noted that, the concentration of Au spheres should be controlled to a very low value to allow an appropriate single particle analysis. Fig. 2b shows a typical dark-field image of an EM-prepared sample, each of the bright spots corresponds to an Au sphere. SERS measurement was made over different particles to obtain a statistical result. Fig. 2c shows typical SERS spectra of PBT obtained in the PBT solution of different concentrations, ranging from 2×10^{-6} to 2×10^{-8} mol L^{-1}. At a further lower concentration, the signal is too weak to detect; and at a higher concentration, the signal is comparable to that at 2×10^{-6} mol L^{-1} and we did not see much increase in the signal intensity.

As can be seen in Fig. 2c, the characteristic Raman peak of the molecule is at 1604 cm^{-1}, and the signal-to-noise ratio of this peak is good enough for single particle SERS detection, even at a concentration as low as 2×10^{-8} mol L^{-1}. We used this peak to perform statistical analysis, and the results are shown in Fig. 2d. The SERS intensity of PBT obtained over OM-prepared particles varied from particle to particle, which was consistent with the multi-dispersed size. In contrast, the signal obtained from EM-prepared Au spheres does not vary as much. For the SERS signal of EM particles, the standard deviation of 2×10^{-8}, 2×10^{-7} and 2×10^{-6} mol L^{-1} PBT are 34.0%, 46.2% and 57.2% respectively, whereas that of OM particles are 68.0%, 81.7% and 82.1%, respectively. Although the average signal obtained from EM-prepared Au spheres is slightly weaker than that from OM-prepared Au spheres at all concentrations, the former obviously gives a better signal reproducibility, pointing to the promising future of single particle SERS analysis.

It has been mentioned above that SERS signals will increase with the increase of the surface roughness or protrusions. To further enhance the SERS signal, we aimed to engineer the microsphere with different roughness features so that the surface roughness can be controlled. It has been reported that a high concentration of reducing agent can promote the formation of sharp tips, which are generally thought to be able to further enhance the local electromagnetic field at the tip.[22,28,32,33] However, increasing the concentration of the reducing agent alone will inevitably change the size of the particles, along with a change of surface roughness due to the variation of the nucleation process. The entanglement between these two aspects is unfavourable for revealing the enhancement mechanism. According to the EM, self-assembly can be suppressed, and all the Au atoms will grow on the given seeds. Therefore, the volume of particles will not change under moderate reaction conditions. As a result, particles with almost the same size, but different surface roughnesses have been successfully prepared simply by varying the concentration of ascorbic acid. The SEM images of four typical roughnesses are shown in Fig. 3a–d. All of them show a very uniform size and surface roughness. The diameters of the particles are in the region of 265 nm. In order to understand how the optical properties of the single particles change with the surface roughness, the single-particle scattering spectra (Fig. 3e) for these four types of Au spheres were collected using a home-made dark-field spectroscopic instrument. The main peak positions of these four spectra are almost the same at 550 nm, which is a typical response of Au spheres. A new peak at around 680 nm is growing and red-shifting with the increase of surface roughness. This peak may be a result of the coupling between the small features under the support of the large Au sphere. Detailed theoretical calculations on these systems will be helpful to locate the ''hot spot'' on such a ''complex'' single particle SERS substrate, which is a topic of another paper.

The single-particle SERS results measured over these Au microspheres are presented as a statistical plot in Fig. 3f. The average intensity of SERS signal increases quite significantly with the surface roughness. The best enhancement factor for the SERS measurement of single particles can be over 5 orders of magnitude (See Appendix for the calculation details). The standard deviation expressed in percentage does not change much with the increase of the surface roughness (a, 32%; b, 35%; c, 34%; d, 23%) (Fig. 3f), and even decreases at the

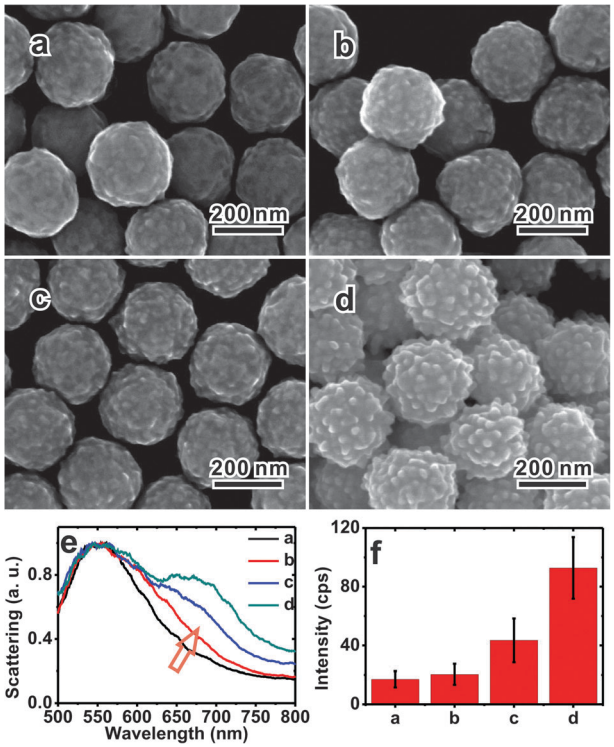

Fig. 3 (a–d) SEM images of EM-prepared Au particles of the same size and increasing roughness. (e) The scattering spectra from these single particles taken from a dark-field CCD. (f) The intensity and the reproducibility of the SERS signal from a single particle of a–d.

roughest surface with the strongest Raman signal. This result points to the promising future of using ''rough'' single Au microspheres for highly reliable single particle SERS detection.

Furthermore, similar to the traditional SM method, the diameter of Au spheres can also be tuned by simply varying the amount of seeds. Indeed, Au spheres with a diameter of 210, 265, 310 and 405 nm were obtained by adding 100, 50, 25, and 10 μL Au seeds, respectively. It is reasonable that we can obtain a smaller particle size at a higher concentration of seeds, as the same amount of Au should be coated over more Au seeds. The SEM images (Fig. 4) of these particles show highly uniform features. A further optimization of the surface roughness over these nanoparticles is now underway, so that they can be used for different laser excitations. Using different metals, such as silver, as the substrate is now also underway.

In summary, we have developed an etching-assisted seed-mediated method to efficiently synthesize highly uniform Au spherical particles using Au nanocubes as the seeds. The particle size can be tuned by the amount of Au seeds. The surface roughness of the particles can be controlled by varying the amount of ascorbic acid. By properly controlling the concentration of particles in the sol to be dispersed on a silicon substrate, we have effectively obtained a highly dispersed Au single particle modified substrate. On the basis of these uniform particles, we combined dark-field microscopy with confocal Raman microscopy to obtain single particle scattering spectra and single particle SERS signals. We have been able to

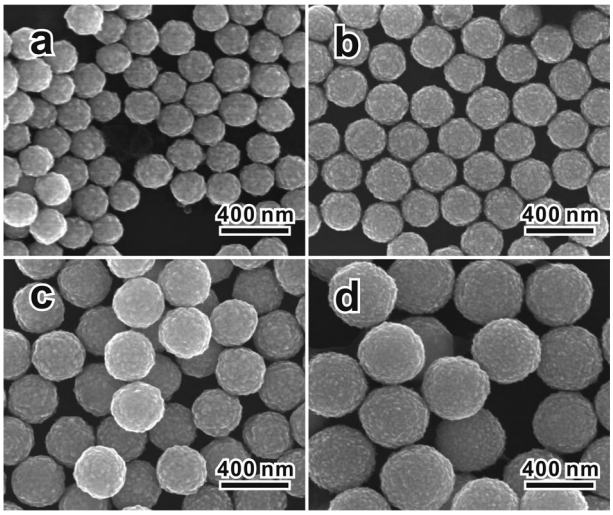

Fig. 4 SEM images of Au spheres prepared using different amount of Au seeds. (a) 100 μL; (b) 50 μL; (c) 25 μL; (d) 10 μL, resulting in diameters of about 210 nm, 265 nm, 310 nm, and 405 nm, respectively.

detect the SERS signal on single particles with a good signal-to-noise ratio for a non-resonant molecule, PBT, even at a concentration as low as 10^{-9} mol L^{-1}. Particles with a rough surface produce a stronger SERS signal, which is crucial for the high sensitivity measurement of weak signals. Furthermore, single particle SERS offers a tool for high throughput measurement because it can collect a large number of data points for the statistical analysis on a sample surface. The high symmetrical nature of single spherical particles offers a new measuring platform for SERS that does not require a good match between the polarization of the laser and the orientation of the SERS particles or substrates. We believe the current advance will be highly important to the practical application of the SERS technique.

Appendix

To estimate the EF of our particles, we chose particles with the roughest surface (Fig. 3d) as a typical case. We estimate the EF according to the expression EF = $(I_{surface}/I_{solution}) \times (N_{solution}/N_{surface})$,[8] where $I_{surface}$ and $I_{solution}$ are the intensities of the SERS signal and reference signal at 1604 cm^{-1}, normalized with the laser power and acquisition time; $N_{solution}$ and $N_{surface}$ are the numbers of PBT molecules probed in the solution and on the surface of one particle.

For SERS experiments, 10 mL sol of as-prepared Au spheres were first washed and then dispersed in 2×10^{-5} mol L^{-1} PBT–ethanol solution and kept undisturbed overnight. This concentration is high enough to ensure a saturated adsorption. A droplet of the mixed solution was dropped onto a quartz slide and covered by another quartz slide with a 0.17 μm thickness. The SERS signal was collected immediately to minimize the evaporation of ethanol.

To acquire the normal Raman signal of the solution, a drop of 1 mM PBT–ethanol solution was injected into a substrate

with groove structures, which was then covered by a quartz slide to form a measuring condition similar to SERS.

The same objective (×50, NA 0.55) was used for SERS and normal Raman measurements. The laser power was 0.8 mW on the sample, and the acquisition time was 30 s for SERS and 8 mW and 100 s for normal Raman measurements. An intensity of 830 and 10 counts per second was achieved in SERS and normal Raman measurements, respectively. After being normalized with the laser power, we obtain $I_{surface}/I_{solution}$ = 830.

To estimate the numbers of PBT molecules probed in the solution, the effective excitation volume (V) should be measured first. $V = \pi(d/2)^2 h$, where d is the equivalent diameter of the laser and h is the equivalent depth of focus (Fig. 5). We measured and calculated d to be 3.6 μm (d is bigger than the SERS experiment with dry particles, which is due to the covered quartz slide and the solution layer):

$$d = \frac{\int_{-\infty}^{\infty} I(x)dx}{I_{max}}$$

h was measured and calculated as 27.5 μm with the formula:

$$h = \frac{\int_{-\infty}^{\infty} I(z)dz}{I_{max}}$$

Thus, the effective excitation volume (V) is calculated to be 280 μm^3, and $N_{solution} = C \times V \times N_A$ is calculated to be 1.7 × 10^8 (C is the concentration of PBT solution). It should be pointed out that such an estimation of the effective excitation volume is much more accurate compared with that reported in the literature using solution or solid samples, in which the Gaussian distribution of the laser power and the different penetration depth in different samples were not considered. Using our method, the evenly distributed laser intensity at both the horizontal plane and vertical direction, the laser diameter and the depth of focus can be presented in an equivalent way. Furthermore, the normal Raman and SERS data should be measured under exactly the same optical configuration.

To estimate the numbers of PBT molecules on a single rough particle, we consider our particle as a big sphere 265 nm in diameter and covered by close-packed 30 nm hemispheres. Thus, we obtain a surface area of about 4.4 × 10^5 nm^2. Suppose each PBT molecule occupies a 0.5 nm^2 area (not the real area, but it will not deviate too much), we obtain $N_{surface}$ to be 8.8 × 10^5.

Considering all the above measured data and the estimated data, we obtain an EF of about 1.6 × 10^5. Although this value is lower than some published EF of single particles (10^6–10^7), we provide here a rather accurate way to estimate the EF: first, we used the equivalent effective extinction volume to estimate the EF; second, we use a non-resonance molecule, PBT, as the probe molecule to avoid any unexpected change in the resonance conditions after binding with the nanoparticle. Therefore, the estimation of EF is more reliable. If we compare the SERS signal with the literature values, which is more significant for SERS applications, the intensities of our signals, after being normalized with the laser power, acquisition time and surface area, are at the same magnitude with other reported single particle results showing a high EF.

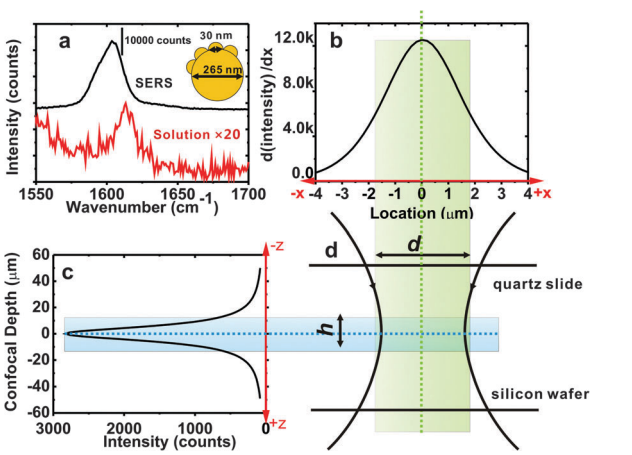

Fig. 5 (a) A comparison between the SERS signal and normal Raman signal. The inset is the model we used to estimate the surface area. (b) The deviation profile of location (x) and intensity (I) of a moving Au pattern in the horizontal plane in water corresponding to (d). (c) The confocal depth (z) and intensity (I) of a moving Si wafer in the vertical direction in water corresponding to (d). (d) The waist profile of a laser beam in solution.

Acknowledgements

This work is financially supported by Ministry of Science and Technology of China (2011YQ03012406, 2013CB933703 and 2009CB930703) and National Science Foundation of China (20825313, 21021120456, 21227004, 21021002, and J1210014).

Notes and references

1 *J. Raman Spectrosc.*, 2005, **36**, pp. 465–747, (Special issue on Surface-enhanced Raman spectroscopy).
2 *Faraday Discuss.*, 2006, **132**, pp. 1–320, (Special issue on Surface-enhanced Raman spectroscopy).
3 *Chem. Soc. Rev.*, 2008, **37**, pp. 873–1076, (Special issue on Surface-enhanced Raman spectroscopy).
4 *Phys. Chem. Chem. Phys.*, 2009, **11**, pp. 7333–7512, (Special issue on Quo vadis surface-enhanced Raman scattering).
5 E. C. Le Ru and P. G. Etchegoin, *Annu. Rev. Phys. Chem.*, 2012, **63**, 65–87.
6 S. Lal, N. K. Grady, J. Kundu, C. S. Levin, J. B. Lassiter and N. J. Halas, *Chem. Soc. Rev.*, 2008, **37**, 898–911.
7 M. J. Natan, *Faraday Discuss.*, 2006, **132**, 321–328.
8 X.-M. Lin, Y. Cui, Y.-H. Xu, B. Ren and Z.-Q. Tian, *Anal. Bioanal. Chem.*, 2009, **394**, 1729–1745.
9 M. J. Banholzer, J. E. Millstone, L. D. Qin and C. A. Mirkin, *Chem. Soc. Rev.*, 2008, **37**, 885–897.
10 M. Moskovits, *J. Raman Spectrosc.*, 2005, **36**, 485–496.
11 E. C. Le Ru and P. G. Etchegoin, *Principles of surface-enhanced Raman spectroscopy: and related plasmonic effects*, Elsevier, Amsterdam, Boston, 2009.
12 H. X. Xu, J. Aizpurua, M. Kall and P. Apell, *Phys. Rev. E*, 2000, **62**, 4318–4324.
13 E. C. Le Ru, P. G. Etchegoin and M. Meyer, *J. Chem. Phys.*, 2006, **125**, 204701.

14 Y. Fang, N. H. Seong and D. D. Dlott, *Science*, 2008, **321**, 388–392.
15 S. M. Stranahan and K. A. Willets, *Nano Lett.*, 2010, **10**, 3777–3784.
16 X. Su, J. Zhang, L. Sun, T. W. Koo, S. Chan, N. Sundararajan, M. Yamakawa and A. A. Berlin, *Nano Lett.*, 2005, **5**, 49–54.
17 K. B. Cederquist, S. L. Dean and C. D. Keating, *Wiley Interdiscip. Rev.: Nanomed. Nanobiotechnol.*, 2010, **2**, 578–600.
18 S. K. Ghosh and T. Pal, *Chem. Rev.*, 2007, **107**, 4797–4862.
19 K. A. Willets and R. P. Van Duyne, *Annu. Rev. Phys. Chem.*, 2007, **58**, 267–297.
20 S. Mahajan, M. Abdelsalam, Y. Suguwara, S. Cintra, A. Russell, J. Baumberg and P. Bartlett, *Phys. Chem. Chem. Phys.*, 2007, **9**, 104–109.
21 A. Tao, P. Sinsermsuksakul and P. Yang, *Nat. Nanotechnol.*, 2007, **2**, 435–440.
22 P. Aldeanueva-Potel, E. Carbó-Argibay, N. Pazos-Pérez, S. Barbosa, I. Pastoriza-Santos, R. A. Alvarez-Puebla and L. M. Liz-Marzán, *ChemPhysChem*, 2012, **13**, 2561–2565.
23 D. V. Goia and E. Matijević, *New J. Chem.*, 1998, **22**, 1203–1215.
24 H. Wang and N. J. Halas, *Adv. Mater.*, 2008, **20**, 820–825.
25 T. K. Sau and C. J. Murphy, *J. Am. Chem. Soc.*, 2004, **126**, 8648–8649.
26 C. Ziegler and A. Eychmüller, *J. Phys. Chem. C*, 2011, **115**, 4502–4506.
27 M. A. Watzky and R. G. Finke, *J. Am. Chem. Soc.*, 1997, **119**, 10382–10400.
28 J. Fang, S. Du, S. Lebedkin, Z. Li, R. Kruk, M. Kappes and H. Hahn, *Nano Lett.*, 2010, **10**, 5006–5013.
29 B. Wiley, T. Herricks, Y. G. Sun and Y. N. Xia, *Nano Lett.*, 2004, **4**, 2057.
30 Y. J. Xiong, J. Y. Chen, B. Wiley, Y. N. Xia, S. Aloni and Y. D. Yin, *J. Am. Chem. Soc.*, 2005, **127**, 7332–7333.
31 B. Schupbach and A. Terfort, *Org. Biomol. Chem.*, 2010, **8**, 3552–3562.
32 E. Hao, R. C. Bailey, G. C. Schatz, J. T. Hupp and S. Y. Li, *Nano Lett.*, 2004, **4**, 327–330.
33 H. You, Y. Ji, L. Wang, S. Yang, Z. Yang, J. Fang, X. Song and B. Ding, *J. Mater. Chem.*, 2012, **22**, 1998–2006.